Journal of Thermal Analysis and Calorimetry, Vol. 66 (2001) 255–264

IDENTIFICATION OF MICRO-SCALE CALORIMETRIC DEVICES
I. Establishing the experimental rules for accurate measurements

V. Torra[1*], *C. Auguet*[1], *J. Lerchner*[2], *P. Marinelli*[3] *and H. Tachoire*[4]

[1]CIRG-DFA-ETSECCPB-UPC, Campus Nord B-4, E-08034 Barcelona, Spain
[2]Inst. Physical Chemistry, T.U. Bergakademie Freiberg, D-09596 Freiberg/Sachsen, Germany
[3]CAB-IB, 8400 S.C. de Bariloche, Argentina
[4]Thermochemical Lab. MADIREL, UP & CNRS, UMR 6121, F-13003 Marseilles CEDEX 03, France

Abstract

The miniaturization of the calorimetric devices to 'nano-sized' scale reduces progressively the available surface of the heat flux detectors with an increase in systematic uncertainty. By means of several Joule and laser signals, the positional effects in 'liquid microcalorimeter' micro-sized chip are evaluated. This allows the introduction of a 3-D coefficient, modifying the standard Joule sensitivity. The shape factor includes the surface and the volume effects.

Keywords: accurate measurements, calibration constant, conduction calorimeters, metrology, nano-sized, position effects, sensitivity, shape factor, systematic errors

Introduction

The conduction calorimeter began in 1930 starting with Tian's calorimeter [1]. Later on, Calvet introduced improvements in the base-line stability and in resolution of the experimental system [2]. Toward 1960 the device became a system of widespread use. Series of modifications and a progressive computerization allow the diversity of current calorimeters that provides results in chemical analysis with relative easiness. Today, it is possible to operate at constant and/or programmable temperature and, even, using complex programming as in the case of AC calorimeters. Following the industrial requirements accurate results are expected and, also, a progressive decrease of the mass quantities of reactants is requested. In fact, a progressive miniaturization of the devices needs an increase of the Seebeck effect. The Fe-constantan, the chromel-constantan, the doped bismuth telluride and Al–Si in the recent flat

* Author for correspondence: E-mail: vtorra@fa.upc.e

1418–2874/2001/ $ 5.00
© 2001 Akadémiai Kiadó, Budapest
Akadémiai Kiadó, Budapest
Kluwer Academic Publishers, Dordrecht

nano-sized calorimeter (Si-based) are the main steps in the last seventy years (from 1930 to 2000) [3–4].

The design conditions have progressively reduced the detector surface. That is, the surface fraction that surrounds the reaction volume and that is endowed with detecting elements has decreased from nearly 80% (in Tian or Calvet classical calorimeters) until, practically zero (only a line of 'warm' junctions) in actual semiconductor devices. This progressive reduction of the detecting surface around the crucible does not affect the reproducibility of the experimental results and does not avoid other difficulties. The uncertainty related to systematic errors or, in other words, the insufficient formulation relating the experimental curves with the intrinsic physical phenomena is a recurrent subject in conduction calorimetry [5]. The misunderstanding between resolution and accuracy by means of conduction calorimeter has produced controversial results. For instance, in shape memory alloys (SMA), a solid-solid phase transition, the calorimetric measurements have produced erroneous interpretations. Several criticisms can be found in literature [6–7].

In the results, obtained via temperature programmed devices, the existence of relevant divergences with sample positioning is relatively easy to be visualized. Figure 1 shows the change in the measured energy determined from the curve surface using a classical equipment: the Differential Scanning Calorimeter 2910 MDSC, TA Instruments, 1997[1]. The measured energy is a function of the radial position of the in-

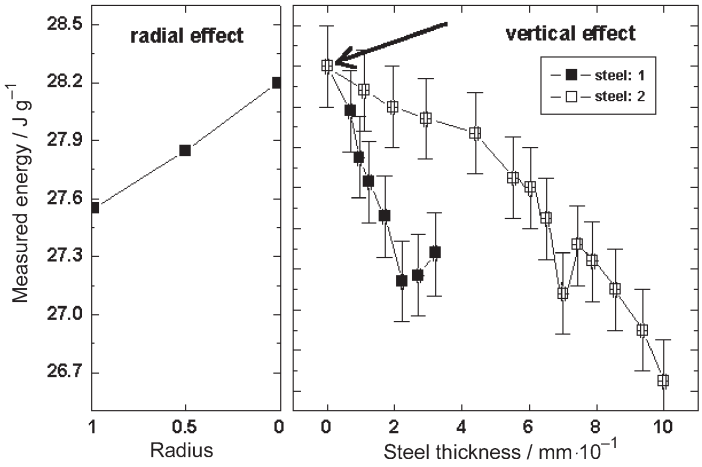

Fig. 1 Calibration procedures in a classical DSC system via melting of an indium sample (19.0 mg) (TA Instrument 2910 MDSC V4.3 B). Scatter of measurements related to the sample positioning. Left: radial changes inside the crucible. Right: dependence with the thickness of the steel slide (situated between the indium sample and the crucible bottom). Open square: cold working on steel slides (one step). Full square: two steps of cold working. Arrow: standard result via the method provided by the manufacturer

1 The operator's manual reads: 'To obtain accurate experimental results you should calibrate each standard DSC cell [...] For the best results [...] For precise experimental results [...] Calibration is performed in instrument's calibration mode, which is accessed through the controller [...].'

dium sample inside the container (Fig. 1 left). Also, the result changes with the z-axis position of the sample. A thin cylindrical slide of memory steel located between the crucible and the indium sample determines the z-axis position. The sensitivity also changes with the previous cold working induced in the steel slide (one or two steps of thickness reduction with ratio of 10:3). Intermediate thickness is obtained via slide polishing. The structural changes probably modify the thermal conductivity. In Fig. 1, the extreme changes of the measured energy with or without a slide of 1 mm thick are close to 7 per cent. The manufacturer's method only furnishes the value indicated by the arrow and the observed differences relate to a systematic uncertainty. In the solid–solid transformations, as SMA, sparse results, related to mass, sample geometry and previous eventual cold working on the samples, are expected.

The differences between the standard calibrations and the intrinsic characteristics of the actual dissipation produce the systematic error. This remains a classical and older discussion clearly recognized in a conference held in Marseilles and realized in 1965[2] but authoritative argument by Calvet stops the discussion[3] [8]. Today, in isothermal as in temperature programmed, the systems reduce their relative detecting surface. For each geometrical, thermal and configuration of the dissipation only a reduced and different fraction of global dissipated heat is detected.

In isothermal work of miniaturized systems several problems converge simultaneously. In the first place, the standard ideas [1–2, 10] need to be modified. The position effects can be visualized and, eventually, systematized to establish experimental rules. Also, from the heat transfer equation (as Fourier equation), the classical elementary models [1–2, 11] can be enhanced. In the second place, other relevant effects related to surface tension, vapor pressure and mixing difficulties need to be quantified. Indeed, the dimensions of the enclosures reduce the mixture processes to diffusive transfer between separate flows as in laminar movement [13]. The energy measurement relates two essential limitations: The reaction is not carried out completely and, also, part of the produced energy moves outside of the detection area by the fluid flow.

The quantification of isothermal measurements in micro-sized calorimeters as XENSOR Liquid Micro Calorimeter (LCM) deposed in a Si-surface [3] behaves to carry out an evaluation of their characteristics in two suitable levels. The first one, inside the reaction volume, the second one, the influences associated with the fluid mechanics. The complete set of the observations presupposes the construction of models that they represent with more correction the characteristics of the experimental systems. A particular thermodynamic model describing each process (i.e. mixture of pure liquids or dilution) is also necessary, for instance [14].

---

2 'Why do you not believe that the calibration using the Joule effect is not totally satisfactory? According to Calvet's book all the phenomena, which are produced within the interior of the calorimeter cell, can be measured with this type of calibration, [...], an excellent calibration is obtained independent of the type of flow distribution in the cell [...] [8].

3 'The same total area will always be obtained independently of the type of thermogram or the distortions occasioned by the variations of the position in the cell's interior, [...] What changes is the form according to the position of the thermal source within the interior of the cell. The effect is important in thermokinetics but in calorimeters it is irrelevant' [8]. See in [9] several comments and criticisms to the Conference Proceedings.

In this work, with metrological target, the link between the sensitivity changes and the position of the energy dissipation is quantified. First at all, using a laser beam, the position dependence on the working surface (x-y coordinates) is analyzed. In a reacting chamber, conceived for continuous mixture analysis, using a Pt resistance, the z-dependence is determined. From the experimental measurements a volume shape factor, modifying the standard Joule calibration suggested by the manufacturer, is established.

Experimental

Two similar experimental equipment based in XENSOR are developed in Barcelona {a} and Freiberg {b}. To analyze the dependence of the position of the dissipation on the chip free surface (x-y coordinates) a conventional red laser pointer has been used (Fig. 2). In {a} two miniature positioning stages from Edmund Scientific (L38-531) or (in {b}) a classical positioning via a microscope plate determines the x-y coordinates of the laser spot on the silicon surface. For each x-y point the resolution is close to 0.2 mm. The laser impinges orthogonal to the silicon surface and the spot area is close to 1 mm^2. The free device (uncovered and without sample) remains in still air. The transmitted and the reflected laser beams are carefully suppressed. The output signal, related to a Heaviside signal in steady state produced by the absorbed beam, is greatly influenced by the photon-electron interactions[4]. This fast and bigger extraneous effects can be avoided by storing the output signal after the input signal is suppressed: the recombination and the storage phenomena related to the photon-electron

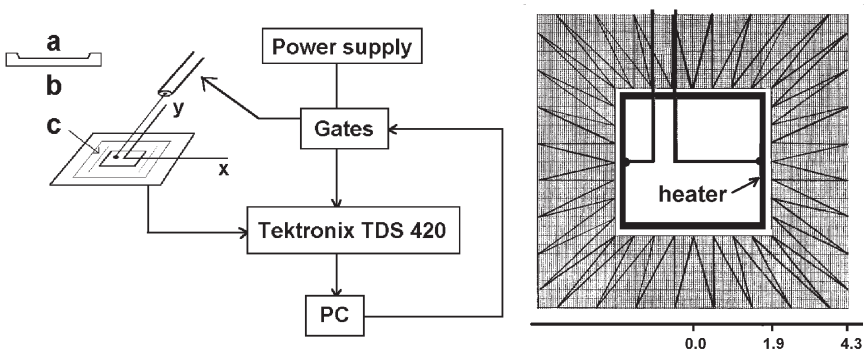

Fig. 2 Left: outline of the experimental set-up based on XENSOR 'Liquid Micro Calorimeter LCM' device and warming via a red laser beam. The output signal is digitized using a Tektronix TDS 420 oscilloscope. a – b) section of LMC;
c) laser beam positioning on available the working surface of LMC. External PC computer controls two gates [12] starting the laser on-off beam and the digitizing command in the oscilloscope. Right: schematic LMC, rear surface; distribution of heater (manufacturer resistance) and thermocouple junctions (scale in mm)

4 To avoid the extraneous photon-electron interactions, several coated chips (furnished by XENSOR) are used without the complete disappearance of relevant photon-electron residual effects. Coating also affects the device dynamics increasing the relaxation time.

effects disappear in 2 or 3 ms. In a free device the disappearance of thermal effects needs some seconds (<6 s). The laser beam is modulated by one on-off computer controlled signal.

Two different digitizing devices of the experimental calorimetric output are used. The first one (sampling 0.0001 s) uses a Tektronix TDS 420 oscilloscope (in {a}). The second one (sampling 0.001 s), for data acquisition and heater control uses a plug-in PC interface board with ADC and DAC (in {b}). The experimental systems are controlled via PC-computers. The fast sampling induces an unfavorable signal to noise ratio. Using series of repetitive measurements, the noise can be reduced via appropriate average.

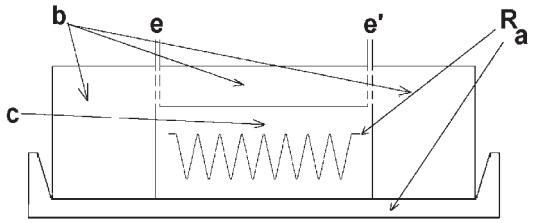

Fig. 3 The z-coordinate analysis in LCM derived devices. Schematic set-up used in liquid–liquid measurements. The cover builds the mixing chamber; squared basis close to 8×8 mm, thickness: 2 mm; a: section of silicon membrane (25 μm thick); b: cover; c: mixing chamber with cylindrical shape, diameter: 4 mm, thick: 1.6 mm; e and e': inlet and outlet; R: heater by platinum wire (thickness: 0.5 mm; z-coordinate position (from silicon membrane): 0.25, 0.75 and 1.25 mm)

In {b} the sensitivity z-dependence was determined in the case of a miniaturized flow-through device [13]. It consists of a silicon chip as described above which is covered by a squared plastic chip with a cylindrical cavity (4 mm diameter, 1.6 mm thick) inside forming the reaction chamber (Fig. 3). The position dependence of the heat sources is determined via small platinum coils (0.5 mm thickness) used as auxiliary heaters. Pt-coil was introduced into the reaction chamber at different distances from the silicon membrane (0.25, 0.75, 1.25 mm). Each change of a heater needs a complete disassemble and reassemble of the device. The chip assembly was mounted into an aluminum block to smooth the room temperature fluctuations. As a sample material, ethanol was filled into the reaction chamber before starting the measurements. In the data acquisition and heater control the {b} the digitizing device is used.

Results

The first part of the analysis relates the heat exchange, via the laser signals directly in the planar silicon device: the x-y or the radial effects. The return to the thermal Heaviside signals, collected 2.5 ms after the laser-off, is position dependent. The sensitivity (or the calibration constant) changes with the distance to the center with a nearly cylindrical symmetry. For several positions of the laser spot, Fig. 4 shows the shape of Heaviside re-

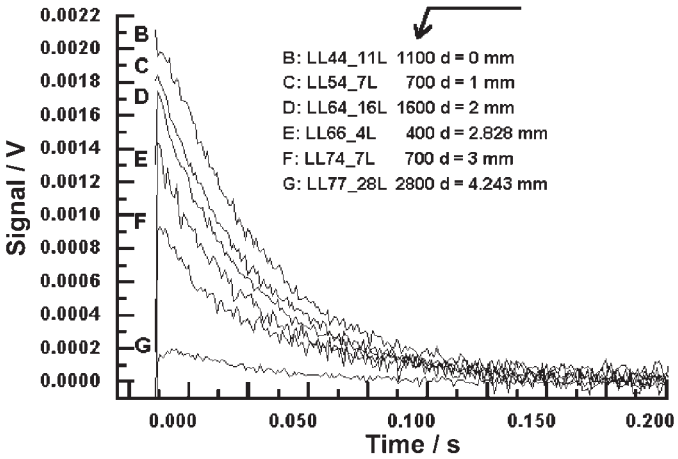

Fig. 4 Heaviside response curves (in voltage *vs.* time) averaged from digitized signals by Tektronix oscilloscope. The signal (B to G) decreases with the distance to the center (d). The arrow shows the number of signals averaged

turns against the distance measured from the center of silicon surface. In Fig. 4, a relevant change of the sensitivity with the laser spot position *vs.* the distance to the center is clearly shown. From B to G curves the thermal Heaviside signal decreases from 2.1 to 0.2 mV. If the working circle is reduced to only 3 mm the extreme values of sensitivity ranges from 2.1 to 0.9 mV. The effective sensitivity relates the effective surface used by the dissipation. In other words, the sensitivity is a function of each actual configuration of the device and/or of experimental measurement.

The shape factor

Figure 5 (left) shows the sensitivity (in reduced units) for several series of measurements realized in different devices and with two available experimental systems. The overall agreement (near 10%) shows 'satisfactory' reproducibility. In other words, the change of the device does not modify the results. In Fig. 5 (right) only a subset of sensitivity values, related to only one device, is used. Also, a roughly polynomial fit, only dependent of the radius, is presented. The four-degree polynomial fit reads,

$$S(r) = a_0 + a_1 r + a_2 r^2 + a_3 r^3 + a_4 r^4 \tag{1}$$

In this particular case, $a_1 a_3 \approx 0$

The fit permits an evaluation of the mean sensitivity S_m, related to a detection inside a circle for a constant thermal power impinging the surface, via

$$S_m = \frac{1}{\pi r^2} \frac{S_J(r=r_J)}{S(r=r_J)} \int_{r=0}^{r=r} S(r) 2\pi r \mathrm{d}r \tag{2}$$

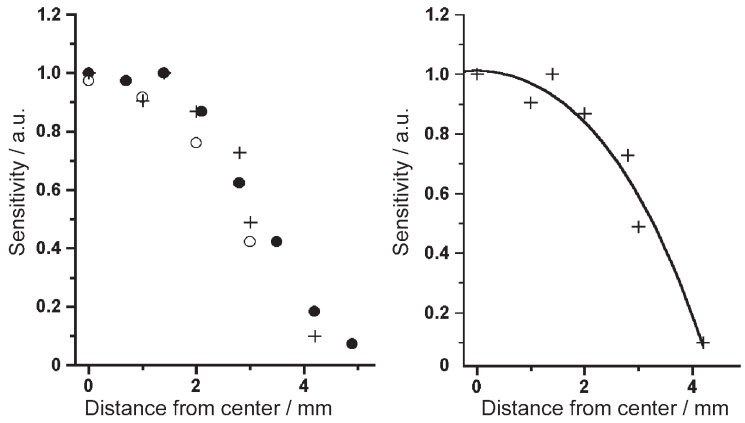

Fig. 5 Laser beam observations. Relative sensitivity *vs.* the distance to center (mm). Left: full and open dots, positioning effects via AD converter; + + + obtained via digital oscilloscope. Right: polynomial fit

S_J is the Joule sensitivity (or standard sensitivity) determined by using the on-chip resistance provided by the manufacturer. In this rough approach the resistance can be considered as an O-ring with radius r_J. S value is the relative sensitivity at the radius r_J determined via the laser beam. S_J/S converts the relative units in the expected V W^{-1} determined by classical Joule calibration (using the on-chip resistance).

In general, a surface shape factor F_{xy} can be defined as,

$$S_m = F_{xy} S_J \tag{3}$$

In a rough hypothesis (cylindrical symmetry), the radial shape factor F_r is defined by,

$$F_r = \frac{1}{\pi r^2} \frac{1}{S(r=r_J)} \int_{r=0}^{r=r} S(r) 2\pi r \mathrm{d}r \tag{4}$$

Using the four-degree polynomial, the mean sensitivity is

$$S_m = 2\frac{S_J(r=r_J)}{S(r=r_J)}\left(\frac{a_0}{2} + \frac{a_1}{3}r + \frac{a_2}{4}r^2 + \frac{a_3}{5}r^3 + \frac{a_4}{6}r^4\right) \tag{5}$$

The 'radial' shape factor F_r can be written as,

$$F_r = \frac{2}{S(r=r_J)}\left(\frac{a_0}{2} + \frac{a_1}{3}r + \frac{a_2}{4}r^2 + \frac{a_3}{5}r^3 + \frac{a_4}{6}r^4\right) \tag{6}$$

Three-dimensional system: the z-dependence

This part of the analysis relates the position effect in the miniaturized flow device outlined in Fig. 3. The device uses a closed chamber and the planar silicon thermo-

pile. The experimental observations relates the practical sensitivity with the effective surface receiving heat and, obviously, with the actual heat power distribution. In the three-dimensional device the used cover and the reactant (i.e. each substance) modifies the heat path. The standard Joule resistance can be considered (the heater in Fig. 2 right) as a squared thinned frame (side: 3.4 mm). The associate mean radius (r_J) (circle with the same surface) can be approached to 1.92 mm. Assuming a heat transfer from the liquid chamber (radius: 2 mm) plus a supplementary effect via the massive squared plastic cover (8×8 mm^2) an effective radius of 3.5 mm needs to be considered. See, below, a tentative approach to match with the extrapolation for z=0. The experimental sensitivity (2.26 V W^{-1}, a point in Fig. 6) determined via the manufacturer resistance needs to be modified to 1.86 V W^{-1} (the + point in Fig. 6) with an estimated uncertainty close to ±5%. The associated shape factor (F_r) value is 0.822 (obtained via the ratio 1.86/2.26). The cover and contents induces relevant changes on the sensitivity and, obviously, in the heat transfer. Their value in a free device – without cover – is close to 2.58 V W^{-1}.

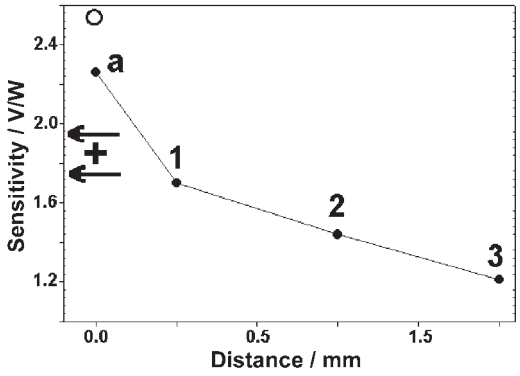

Fig. 6 Sensitivity changes with the position of heater in the z-axis. o: standard sensitivity related to free device. a: standard sensitivity (2.26 V W^{-1}) using cover and content. 1, 2 and 3 experimental values (1.70, 1.44 and 1.21 V W^{-1}) established via the three platinum resistances. +: extrapolated value (1.86 V W^{-1}) at z=0. Associated shape factor value F_r close to 0.822 V W^{-1}. The arrows show the expected uncertainty on the + value

Figure 6 shows the direct experimental results of the sensitivity *vs.* the z-axis (chamber contents ethyl alcohol). Point 'a' relates the classical Joule or 'standard' Joule effect in the used configuration and in the on-chip resistance. 1, 2 and 3 are the Joule sensitivity measurements deduced from the three-platinum wire resistance. The z-effect (1, 2 and 3) creates, practically, a straight line. The extrapolation (to z=0, + point) does not match with the standard Joule (point 'a').

The volume shape factor $F_{(V)}$ and the standard Joule sensitivity determines the volume 'mean sensitivity' $S_{(V)}$ via:

$$S_{(V)}=F_{(V)}S_J=F_zF_{xy}S_J \quad (7)$$

In the radial approximation

$$S_{(V)}=F_{(V)}S_J=F_zF_rS_J \quad (8)$$

Figure 6 shows that the z-action can be considered close to a linear effect. Their mean value is practically similar to the point 2 situated in the center of the z-length (from z=0 to z=1.6 mm). The F_z value remains close to 0.774 or, in this case, the ratio between sensitivity in the point 2 divided by the sensitivity in the point + or 1.44/1.86. The value of $F_{(V)}$ (volume shape factor) is close to 0.636.

Conclusions

In nano-sized devices the standard calibration using a Joule calibration system furnished by the manufacturer produces systematic errors. An evaluation of the position effect via a laser beam and several Joule effects permits the determination of the volume shape factor $F_{(V)}$ and the formulation of two shape factors (F_{xy} and F_z) related to surface and to z-axis. From the volume shape factor a reduction of systematic differences can be expected. In the used system, the volume shape factor induces relevant changes (nearly 40%) in the standard Joule calibration.

Remark

Experimental measurements establish the existence of relevant changes on the sensitivity with the heat source position and the experimental configuration. In other words, the standard methods to determine the sensitivity, usually furnished by the manufacturer (free device: 2.58 V W^{-1}, with cover and containing ethanol: 1.86 V W^{-1}), need to be improved for each used configuration. In fact, the progressive reduction of the detecting surface increases the systematic errors without shifts in statistical errors. The estimated uncertainty on the shape factor relates the position errors on the measurements. For instance, the resistance position is used to extrapolate at z=0. The uncertainty in z-coordinate is close to 0.1 mm (points 1, 2 and 3 in Fig. 6). Roughly the error on $F_{(V)}$ can be estimated close to ±5%.

* * *

The work was carried out in the frame of integrated actions HA 1999-0087 (MCT-Spain) and 314-Al-e-dr (DAAD, Germany) between Freiberg and Barcelona group, and ACI99-2 and 6 (Gen. Cat.) between Barcelona with Marseilles and with S. C. Bariloche groups. Also, the ACES 1999-00040 (Gen. Catalonia) related to nanocalorimeters is gratefully acknowledged. P. M: acknowledges a predoctoral grant from CNEA (Centro Atómico Bariloche, Argentina).

References

1 A. Tian 'Recherches sur la calorimètrie par compensation. Emploi des effets Peltier et Joule. Étude d'un microcalorimètre intégrateur, oscillographe et balistique', L. JEAN, Imprimeur, Gap, 1931.

2 E. Calvet and H. Prat, Microcalorimétrie, Masson 1956.

3 Liquid micro calorimeter by Xensor Integration, Delft, The Netherlands (website: www.xensor.nl).
4 J. M. Köhler, E. Kessler, G. Steinhage, B. Gründig and K. Cammann, Microchim. Acta, 120 (1995) 309.
5 J. E. Callanan, J. Thermal Anal., 45 (1995) 359.
6 V. Torra and H. Tachoire, Thermochim. Acta, 203 (1992) 419.
7 P. Wollants, J. R. Roos and L. Delaey, Prog. Mater. Sci., 37 (1993) 227.
8 Microcalorimétrie et Thermogenèse, n°156, Éditions du Centre National de la Recherche Scientifique, Paris 1967.
9 V. Torra and H. Tachoire, J. Therm. Anal. Cal., 52 (1998) 663.
10 P. Dantzer and P. Millet, Rev. Sci. Instrum., 71 (2000) 142.
11 S. C. Mraw, Rev. Sci. Instrum., 53 (1982) 228.
12 F. Moll, private communication (2000).
13 J. Lerchner, A. Wolf, A. Weber, R. Hüttl, G. Wolf, J. M. Köhler and M. Zieren, Proc. of 3th International Conference on Microreaction Technology, 18-21/04/1999, Frankfurt/Main, Germany 1999.
14 H. Tachoire and V. Torra, Thermochim. Acta (Thermal Analysis Highlights 8th ICTA), 110 (1987) 171.